

OPTIMIZATION OF AIR FLOW THROUGH A HEAT EXCHANGER IN AN AUTOMOTIVE HVAC

¹Vivek A. Jairazbhoy, ¹LeeAnn Wang, ¹Mehran Shahabi, ²Ravi Nimbalkar and ²Sunil Earla

¹Automotive Components Holdings, USA, ²BETA CAE Systems USA, USA

KEYWORDS – Shape Optimization, Airflow, HVAC, ANSA, Morphing

ABSTRACT – Heat Exchanger performance in an automotive HVAC is critically influenced by the uniformity of flow through the core face on the air side. Performance is generally measured in terms of both Core Duty and Pressure Drop. HVAC units are typically tightly constrained by packaging requirements imposed on components under the Instrument Panel resulting in maldistribution of flow across typical cross-sections. In order to improve heat exchanger performance, such maldistribution upstream of the device must be rectified without infringement of packaging boundaries.

In this paper, we show how vanes, or baffles, may be used in automotive HVAC units to achieve certain objectives relating to flow uniformity upstream of heat exchangers. CFD is used as a means of capturing the impact of design changes on performance objectives. A "guide vane" with qualitatively desirable characteristics is parameterized, and the ANSA morphing capability used to introduce the parameterized feature into the flow domain. The parametric representation permits examination of the design space in search of optimum solutions with respect to the objectives. Formal optimization methods are used to drive the solution search. ANSA™ is used for morphing and meshing, FLUENT® is used to perform CFD, and iSIGHT-FD™ is used for all optimization algorithms.

1. INTRODUCTION

The design and engineering of an automotive HVAC involves an in depth understanding of the flow of air through the system. Fresh air from the cowl is drawn into the inlet chamber the HVAC by a blower located just downstream of the chamber. In certain modes of operation, recirculated air from the cabin can also feed into the inlet chamber. Centrifugal effects in the blower scroll generate a significantly non-uniform flow at the blower exit. To ensure thermally efficient operation of the evaporator core located inches downstream of the blower exit, flow non-uniformities must be minimized before the air passes through the core. Since the cross-section of the core is much larger than that of the blower exit, a diffuser section is designed between the two cross-sections. After passing through the core, the air is directed through one or more of several parallel paths aimed at distributing it between distinct outlets and, in some instances, heating it.

From a fluid mechanical standpoint, the diffuser region is arguably the most critical section of an automotive HVAC. Functionally, this section must be designed to meet the following requirements:

1. A certain minimum level of flow uniformity to ensure effective use of the heat transfer surface associated with the evaporator.
2. A means for accomplishing highly efficient pressure recovery.
3. An acceptable level of aerodynamic noise.

An effective way to control the flow in the diffuser is by means of appropriately designed baffles or "vanes" located within selected regions of the diffuser [1]. The present study undertakes to develop a method to optimize the location and shape of a single such vane to maximize

uniformity and pressure recovery in the diffuser. Generally, effective pressure recovery and low aerodynamic noise go hand in hand.

2. METHODOLOGY DEVELOPMENT

In this paper, we present a procedure to search for an optimal design for an automotive HVAC diffuser. The design variables arise from selected parameterized geometric features within the diffuser. The constraints are derived from the condition that the parameterized geometric features must not violate certain design rules and packaging bounds, while the design objectives include:

1. Maximization of Evaporator Coverage, defined as the percentage of the evaporator core surface area that experiences air velocities $\pm 20\%$ from the mean.

Mathematically, Evaporator Coverage (E) may be represented as:

$$E = \{\text{Area}(0.8v_{\text{avg}} < v < 1.2 v_{\text{avg}})\} / \{\text{Total Evaporator Face Area}\} \quad \dots\dots (1)$$

2. Maximization of pressure recovery defined as:

$$\Delta P = \{\text{Avg static pressure at evaporator inlet} - \text{Avg inlet static pressure}\} \quad \dots\dots (2)$$

The scheme relating to the formal optimization of geometric features in a CFD model to maximize certain performance criteria has precedence in the literature [2]. However, the optimal design procedure proposed in this paper is unique in certain ways and involves the following steps:

1. Begin with a baseline design that provides an outer contour for the diffuser, but has no vanes. The design may represent the best guess of an automotive HVAC design engineer, or more desirably, emerge from a separate study relating to the optimization of the wall contours of the diffuser. It is of interest that, in this study, the baseline chosen is mature one – i.e. one that has already undergone numerous "manual" iterations pertaining to the exterior geometry. Each iteration consists of (a) a CFD run, (b) a results evaluation, and (c) the development of an ad hoc means to improve the result. The objective is to improve the design beyond that achieved by conventional methods.
2. Execute a CFD study of the flow in the baseline diffuser under specified conditions. Extract the following information from the study:
 - a. Velocity contours on the surface of the evaporator core. The intent is to understand which areas of the core are subjected to excessive flow, and which areas have unacceptably low flow.
 - b. Evaporator Coverage as defined by equation (1).
 - c. Pressure Recovery as defined by equation (2).
3. From the information in Step 2, identify a conceptual vane shape and approximate location aimed toward effective redistribution of the flow over the evaporator surface.
4. Devise a quantitative parametric representation of the vane shape and location using a sufficient number of design variables to capture the design intent, yet not too many that would render the optimization problem intractable. Also represent the constraints in terms of the design parameters. Later in this paper, we explain this step in more detail.
5. Devise a means to introduce the parametric representation of the vane into the baseline ANSA model. Hence use the ANSA morphing capability to create a volume mesh. Capture the repetitive tasks used to accomplish Step 5 in an ANSA "Task Sequence"

that may be operated in batch mode while being called repeatedly by iSIGHT-FD, the optimization tool.

6. Devise an iSIGHT-FD driven algorithm to conduct a Design of Experiments (DOE) that explores the parameter space while producing values of the design objectives for each DOE run. The algorithm should call the following modules in sequence:
 - a. A design parameter processing module (an Excel™ spreadsheet, in this study) that produces input for the ANSA Morphing and Task Sequence.
 - b. ANSA, to execute the parameterization and volume meshing steps.
 - c. FLUENT, to execute the CFD run that resolves the flow field in the domain and hence produces values of the design objectives.
7. Develop a procedure to filter the DOE matrix with the constraints so that only models containing vanes lying wholly in feasible space are executed.
8. Run the DOE, and create Response Surface Models (RSM) for each of the design objectives.
9. Execute a Multi-Objective Optimization scheme in iSIGHT-FD using the RSM's to explore the parameter space for optimum solutions.

3. PROBLEM SETUP

Step 1: Baseline design

In the current study, we assume that the baseline design is provided.

Step 2: Baseline CFD study

Figure 1(a) shows velocity contour plots at the evaporator core surface. The mean velocity is 2.47 m/s. Figure 1(b) shows "clipped" contours, the "white" areas indicating regions in which the velocity is either less than $0.8v_{avg}$, or greater than $1.2 v_{avg}$ (see equation 1). The Evaporator

Coverage as defined by equation (1) is 78.5%. The Pressure Recovery as defined by equation (2) is 108.3 Pa.

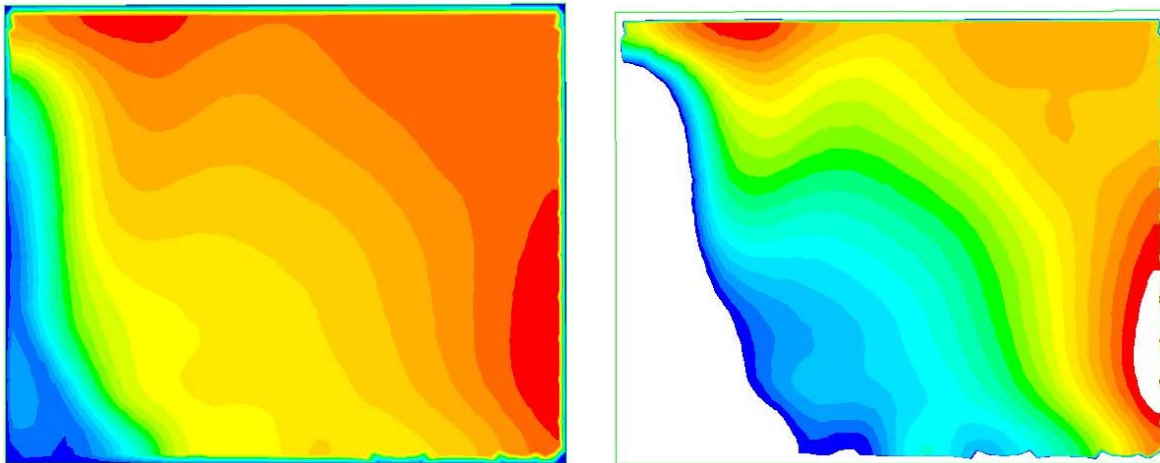


Figure 1(a): Velocity Contours at Evaporator; Figure 1(b): Clipped Velocity Contours

Step 3: Conceptual vane shape and approximate location

Figure 2 shows velocity vectors in the baseline model of the diffuser flow. As the flow turns anticlockwise from the inlet towards the evaporator, centrifugal effects force the air to the outside, flooding the right side of the evaporator (as seen from upstream) while starving the left side. The conceptual vane shape and approximate location required to fix the maldistribution is shown in Figure 3.

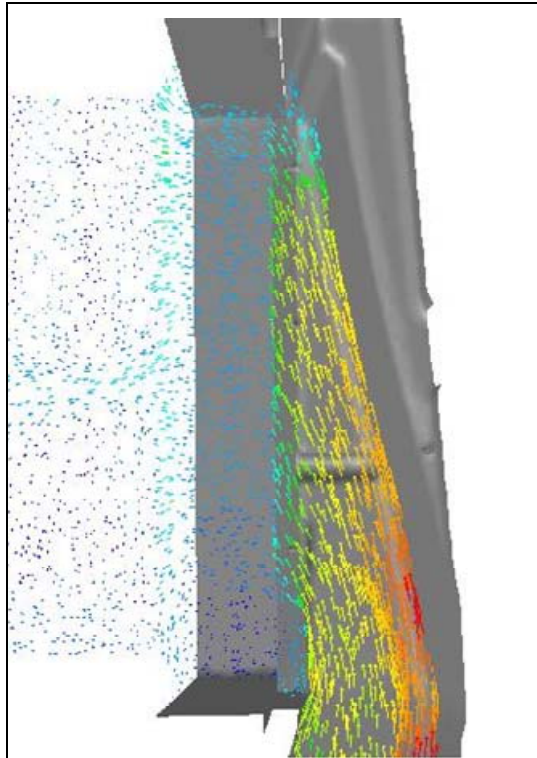


Figure 2: Baseline Flow;

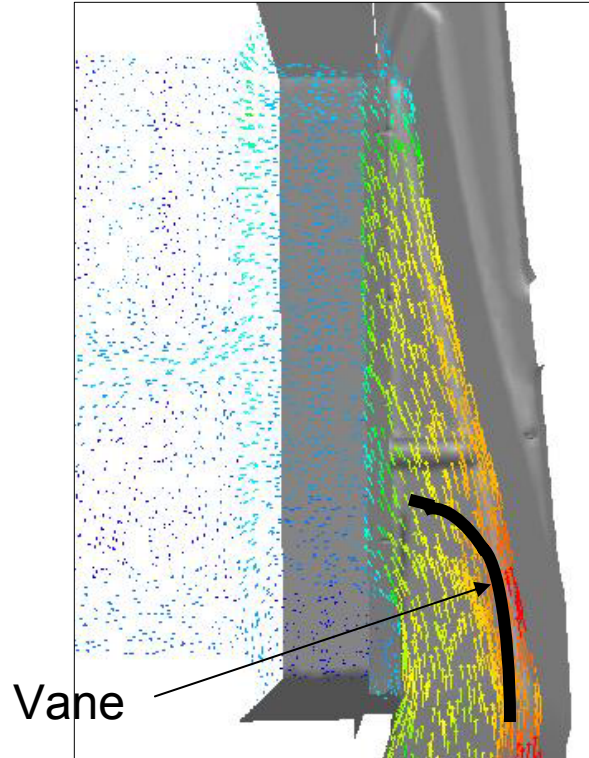


Figure 3: Conceptual Vane Shape

Step 4: Parameterization

$\beta(\text{deg})$	Angle subtended by Arc 1 at Center 1
$\gamma(\text{deg})$	Angle subtended by Arc 2 at Center 2
d	Trailing linear segment
R_1	Radius of Arc 1
R_2	Radius of Arc 2
x_i	x-coordinate of inlet
y_i	y-coordinate of inlet

Table 1: 7-Parameter System

There are innumerable ways to represent an essentially C-shaped vane in the manner discussed. In order to render the problem tractable yet representative, we select a 7-parameter system describing the shape and location of the vane (Figure 4). The shape is produced by

extruding a 2D curve consisting of 2 contiguous arcs, each with its own radius, aimed at redirecting flow towards the low velocity areas of the core, followed by a downstream linear segment aimed at straightening the flow to reduce recirculation. The 7 parameters are defined in Table 1.

Next, we represent the extrudable 2D shape of the vane in terms of the parameters. We begin by defining a coordinate system with its origin at the leading edge of the vane, as shown in Figure 4. The vane is represented by the 3-segment curve OACD consisting of two arcs of different radii (OA and AC) followed by a linear segment (CD). In order to represent the vane parametrically, we need accomplish the following tasks:

1. Find the coordinates of the centers, O_1 and O_2 , of the circles from which the arcs can be created and the coordinates of the points A, B, C, and D.
2. Express all coordinates in terms of the design parameters.

Parametric Representation

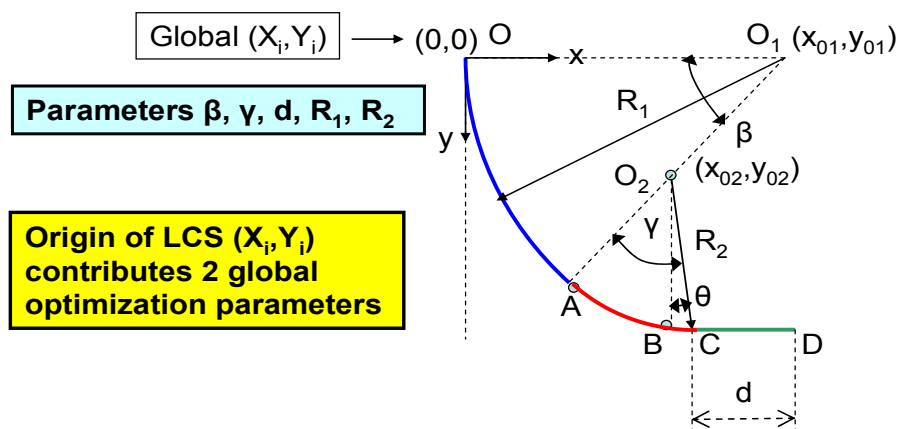


Figure 4: Parametric Representation of the Vane

From Figure 4, the following relationships are apparent:

$$x_A = 2R_1 \sin^2(\beta/2) \dots\dots\dots (3)$$

$$y_A = R_1 \sin^2 \beta \dots\dots\dots (4)$$

$$x_{o1} = R_1 \dots\dots\dots (5)$$

$$y_{o1} = 0 \dots\dots\dots (6)$$

$$x_{o2} = R_1 - \Delta R \cos \beta \dots\dots\dots (7)$$

$$y_{o2} = \Delta R \sin \beta \dots\dots\dots (8)$$

$$x_B = R_1 - \Delta R \cos \beta \dots\dots\dots (9)$$

$$y_B = R_2 + \Delta R \sin \beta \dots\dots\dots (10)$$

In the above expressions, ΔR is defined as

$$\Delta R = R_1 - R_2 \dots\dots\dots (11)$$

Define

$$\theta = (\beta + \gamma - \pi/2) \dots\dots\dots (12)$$

Hence

$$x_C = x_B + R_2 \sin \theta \dots\dots\dots (13)$$

$$y_C = y_B - R_2 + R_2 \cos \theta \dots\dots\dots (14)$$

$$x_D = x_B + R_2 \sin \theta + d \cos \theta \dots\dots\dots (15)$$

$$y_D = y_C - d \sin \theta \dots\dots\dots (16)$$

In global coordinates, the coordinates of the point D can be expressed as follows:

$$x_E = x_i + x_D \quad \dots\dots\dots (17)$$

$$y_E = y_i + y_D \quad \dots\dots\dots (18)$$

Bounds for the DOE associated with each of the input variables are listed in Table 2. The endpoint of the vane must lie in feasible space. This condition is applied as a constraint on the endpoint coordinates, also shown in Table 2. These constraints will be used in Step 7 to filter the DOE, thus requiring computationally intensive CFD to be applied only to feasible points.

BOUNDS*		
Parameter	Min Value	Max Value
β (deg)	5.0	30.0
γ (deg)	40.0	80.0
d	2.0	10.0
R_1	40.0	220.0
R_2	6.0	30.0
x_i	0.0	19.1
y_i	-0.2	17.3
CONSTRAINTS*		
x_E	6.0	37.0
y_E	20.0	120.0

* All length units in mm

Table 2: Bounds and Constraints

Step 5: ANSA model with parameterized vane

In this step, we develop a means to introduce the parametric representation of the vane into the baseline ANSA model, using morphing for shape manipulation.

We begin by creating a base model with morphing boxes set up to modify the shape of the vane parametrically. To run the shape optimization in batch mode, we define an optimization task in ANSA Task Manager. The optimization task is populated with the required number of Design Variable items and each design variable is linked to the respective morph parameter. A design Variable input file, which acts as an adapter file between ANSA and the Optimizer, is created as a child item in the task. The "Current Value" field in the design variable file, which provides input values for the design variables, is updated at each function call. The input provided through the design variable file drives the morphing parameters in the base model (Figure 5).

The screenshot displays the ANSA software interface. On the left is the 'Tasks View' showing a hierarchical tree of tasks. A red arrow points from the 'INPUT_DV.txt' file in the tree to the 'DESIGN VARIABLES' table. Another red arrow points from the 'Translate_box_2_in_X' task in the tree to the 'PARAMETERS' dialog box. A third red arrow points from the 'Scripts & Session Commands' label to the 'PARAMETERS' dialog box.

DESIGN VARIABLES

# ID	DESIGN VARIABLE NAME	TYPE	RANGE	CURRENT VALUE	MIN VALUE	MAX VALUE
1	Radius_box_1	REAL	BOUNDS,216.36, -1000., 1000.			
2	Translate_box_1_in_X	REAL	BOUNDS,182.34, -1000., 1000.			
3	Translate_Box_1_in_Y	REAL	BOUNDS,5.1, -1000., 1000.			
4	Change_in_Arc_1_Length_After_Radius_Change	REAL	BOUNDS,-148.5554865, -1000			
5	Radius_box_2	REAL	BOUNDS,6.97, -1000., 1000.			
6	Rotation_of_2D_Box_2	REAL	BOUNDS,-39.34, -180., 180.			
7	Translate_box_2_in_X	REAL	BOUNDS,-13.58424947, -1000., 1000.			
8	Translate_box_2_in_Y	REAL	BOUNDS,78.97733462, -1000., 1000.			
9	Change_in_Arc_2_Length_After_Radius_Change	REAL	BOUNDS,-0.565669937, -1000			
10	Rotation_of_Linear_Segment	REAL	BOUNDS,-43.99, -180., 180.			
11	Translate_box_3_in_X	REAL	BOUNDS,-35.26926469, -1000., 1000.			
12	Translate_box_3_in_Y	REAL	BOUNDS,51.09957388, -1000., 1000.			
13	Change_in_Length_of_Linear_Segment	REAL	BOUNDS,-2.747, -1000., 1000.			

PARAMETERS

Name	Type
1 Radius_box_1	RADIUS
2 Translate_box_1_in_X	TRANSL
3 Translate_Box_1_in_Y	TRANSL
4 Change_in_Arc_1_Length_After_Radius_Change	LENGTH
5 Radius_box_2	RADIUS
6 Rotation_of_2D_Box_2	ROTATE
7 Translate_box_2_in_X	TRANSL
8 Translate_box_2_in_Y	TRANSL
9 Change_in_Arc_2_Length_After_Radius_Change	LENGTH
10 Rotation_of_Linear_Segment	ROTATE
11 Translate_box_3_in_X	TRANSL
12 Translate_box_3_in_Y	TRANSL
13 Change_in_Length_of_Linear_Segment	LENGTH

Scripts & Session Commands

Figure 5: Task Tree

The base model with two circular and one straight FE vane section is created. Morphing boxes are set up for all vane sections to modify their shapes parametrically. Cylindrical and 2D morphing boxes are used to accomplish the desired shape change. The morphing boxes are parameterized using ANSA morphing parameters such as Translate, Rotate, Length, and Radius.

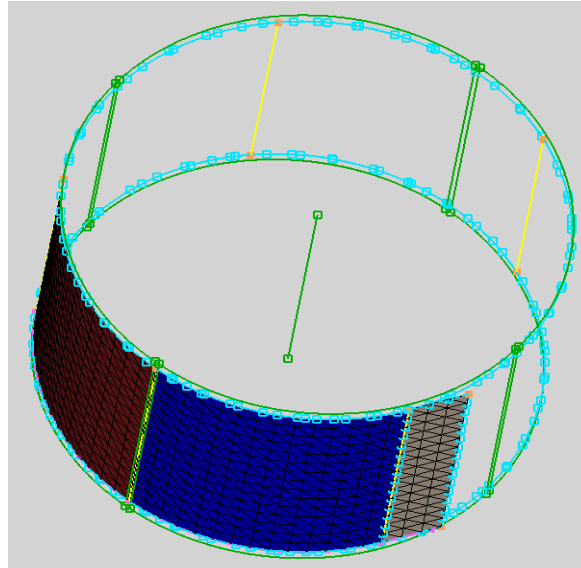


Figure 6: Cylindrical Morphing Box

The Box-in-Box morphing concept is used when 2D morphing boxes are loaded to cylindrical morphing boxes, in addition to the vane sections. Thus, a change in the radius of the cylindrical boxes would morph the 2D morph boxes to the new radius along with the vane sections.

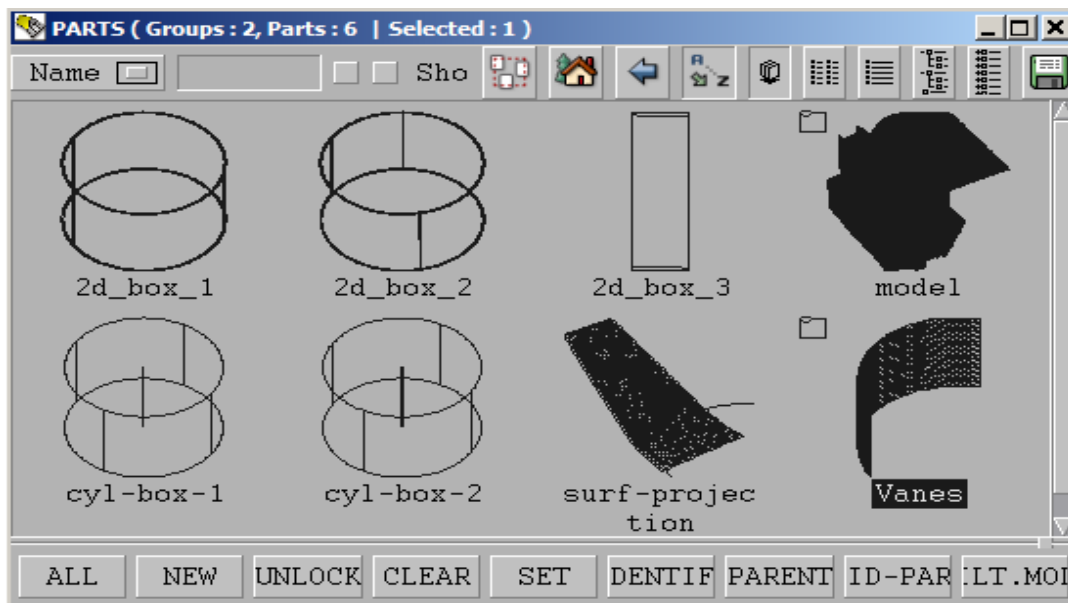


Figure 7: Key Morphing Entities

Once the radius changes are performed the 2D boxes perform the length change for the vane sections. Finally, the "translate" and "rotate" parameters relocate and reorient the vane sections to make a complete continuous vane assembly.

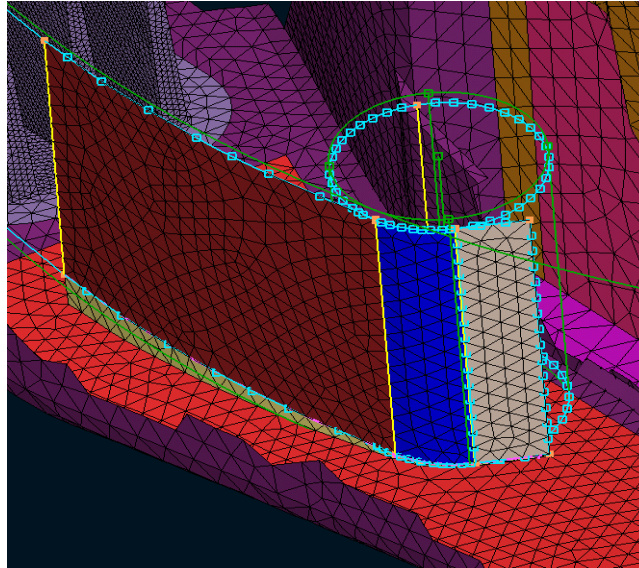


Figure 8: Morphed Vane Shape

Connection lines are used to make the connections between morphed vane sections and the surface onto which the vanes project.

Certain subtasks, such as connecting vane sections to the projection surface, reconstructing the morphed mesh, and isolating parts to define the volume, require user defined scripts. These subtasks are implemented using the ANSA scripting functionality. ANSA session commands are also used through the task sequence to paste nodes automatically, to connect individual vane sections to each other in their final morphed state, to create a solid tetra mesh, to write output in Fluent format, etc.

The eventual task sequence is driven by the optimizer in a no-gui batch mode with no user interaction.

Step 6: Filtered Optimal Latin Hypercube Method

Execution of the DOE discussed earlier requires the generation of a design matrix. Several DOE method options are available in iSIGHT-FD such as Full Factorial, Orthogonal Array, Latin Hypercube, Optimal Latin Hypercube, etc. The traditional Optimal Latin Hypercube Method has the ability to distribute DOE points evenly within the n-dimensional space defined by the n factors associated with a given DOE, allowing higher order effects to be captured and more combinations to be studied for each factor. However, constraints which are complex functions of one or more factors cannot be directly accounted for in the method. For this reason, we develop a "*Filtered Optimal Latin Hypercube Method*" in this paper.

We begin by expressing each constraint in the form:

$$f(x_1, x_2, \dots, x_n) \leq 0 \quad , \text{ where} \\ \dots\dots\dots (19)$$

$x_1, x_2 \dots x_n$ are factors.

Next, a design matrix is generated in iSIGHT-FD™ and filtered against the constraints expressed in the form of equation (19). The resultant filtered matrix is, typically, well distributed in the "interior" of the constrained domain, but could exhibit some unevenness in the distribution in the proximity of the constraints. The advantage of this method is that all CFD models executed contain vanes lying wholly in feasible space.

Step 7: Design of Experiments (DOE)

The next step is to devise an Optimizer driven algorithm to conduct a Design of Experiments (DOE) that explores the parameter space while producing values of the design objectives for each DOE run. This step is executed in two stages:

1. An Excel™ spreadsheet is created that, using equations (3) through (16) and the procedure outlined in Step 5, takes the 7 design variables on input and creates quantitative information in the form of 13 intermediate variables required to execute the ANSA tasks described in Step 5. The Excel™ spreadsheet is called by iSIGHT in a loop over the filtered design matrix, as shown in Figure 5, creating a text file containing the ANSA inputs for each feasible CFD model.

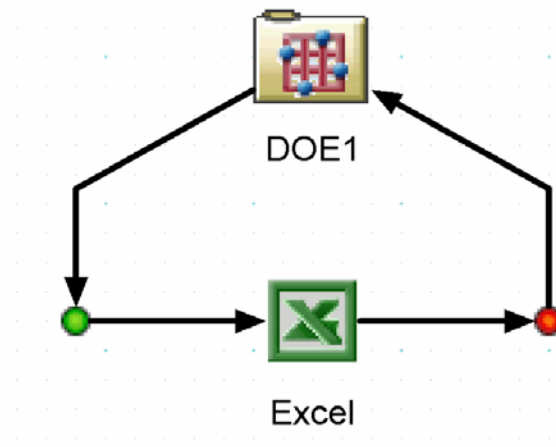


Figure 8: Creation of ANSA Task inputs for the DOE

2. Next, a DOE loop is set up in iSIGHT that executes calls to ANSA and Fluent sequentially, using the ANSA inputs generated by the Excel™ spreadsheet described earlier in Step 7. The filtered DOE matrix consists of 59 feasible guide vane configurations. The DOE batch loop links relevant outputs of the meshing tool ANSA to the input deck of the CFD solver Fluent. Figure 9 depicts the batch loop.

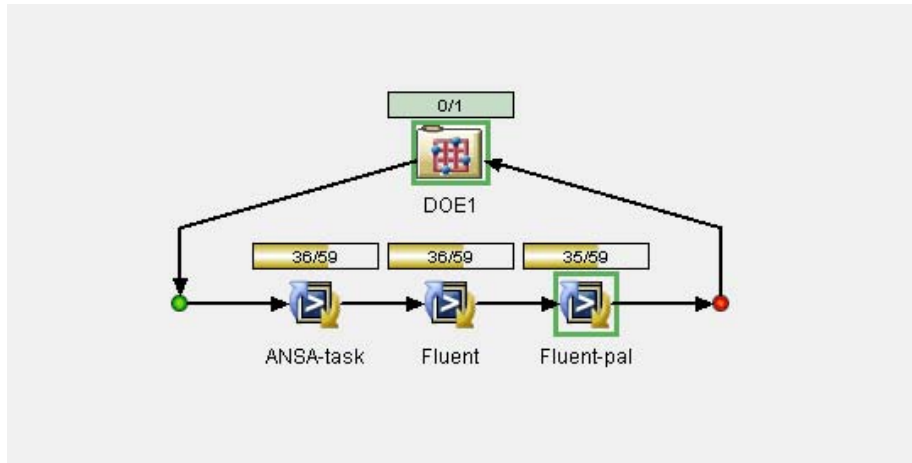


Figure 9: DOE Batch Loop

The Task-driven ANSA morphing technique explained in Step 5 is executed to create feasible guide vanes for each of the 59 entries in the DOE design matrix. The input to ANSA consists of the 13 intermediate variables generated from the 7 design variables by the Excel™ spreadsheet. A volume mesh for the whole flow domain is generated as an output of each ANSA run. The volume mesh is then input into the CFD solver Fluent.

For each DOE run, the boundary conditions, the solver control parameters and the turbulence modeling information in Fluent are set up for the HVAC flow domain containing the new vane shape through a journal file. The parameters used to compute evaporator coverage are extracted from the converged Fluent results at the end of each DOE run.

Step 8: Response Surface Models

Since each CFD "function call" is computationally intensive, searching with such function calls within a 7-parameter design space for an optimum can be very expensive. The practical solution to this difficulty is to create a Response Surface Model (RSM) approximation of the DOE data generated in Step 7 based on a polynomial fit via a least squares regression of the output

parameters to the input parameters. iSIGHT provides an "Approximation" component that facilitates the creation of such an approximation.

Step 9: Multi-Objective Optimization (NCGA)

Since the diffuser must be designed to maximize more than one objective, Multi-Objective Optimization is an effective means to examine the design problem. iSIGHT-FD offers a Multi-Objective Exploratory Technique called the Neighborhood Cultivation Genetic Algorithm (NCGA) in which each objective is treated separately [3]. A Pareto front can be generated by selecting feasible non-dominated designs. The NCGA algorithm is used in this paper.

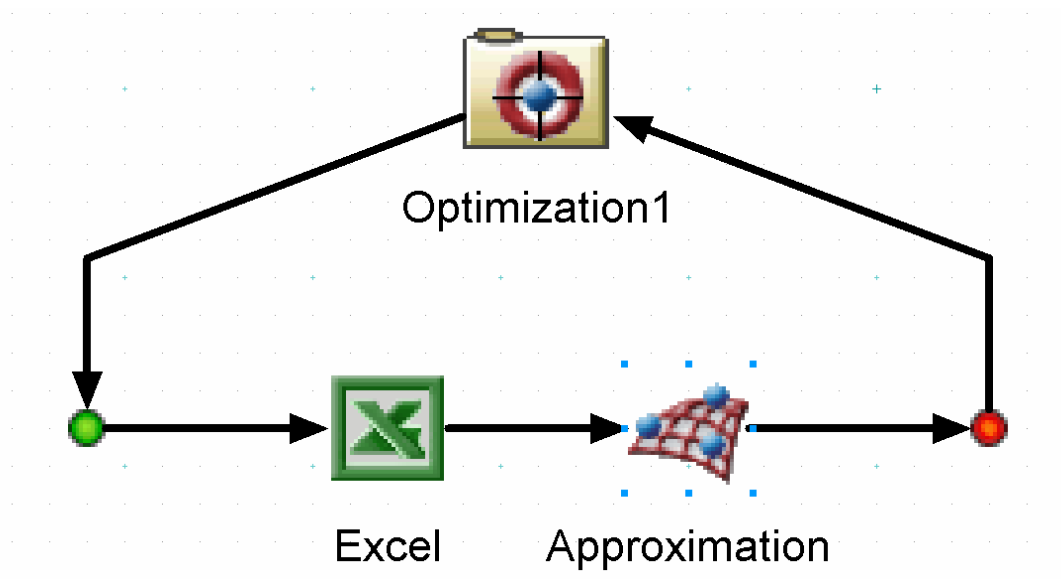


Figure 10: Optimization Using the RSM Approximation

Figure 10 depicts the loop in which the Optimizer (NCGA algorithm) drives an Excel[™] spreadsheet that calculates the constraints, followed by a component that computes the design objective values using the RSM approximation generated in Step 8. The results can then be processed for feasible non-dominated solutions using Pareto Front scatter plots.

4. RESULTS AND DISCUSSION

Using a cubic RSM approximation, the loop depicted in Figure 10 is executed for 5000 function evaluations. The infeasible designs and designs yielding evaporator coverage numbers of less than 80% are filtered out. The remaining data are examined from the standpoint of sensitivity and optimality.

The sensitivity of both objectives to variations in the design variables is shown in Figure 11. The blue points shown lie on the Pareto front and hence represent candidate optimal (non-dominated) designs.

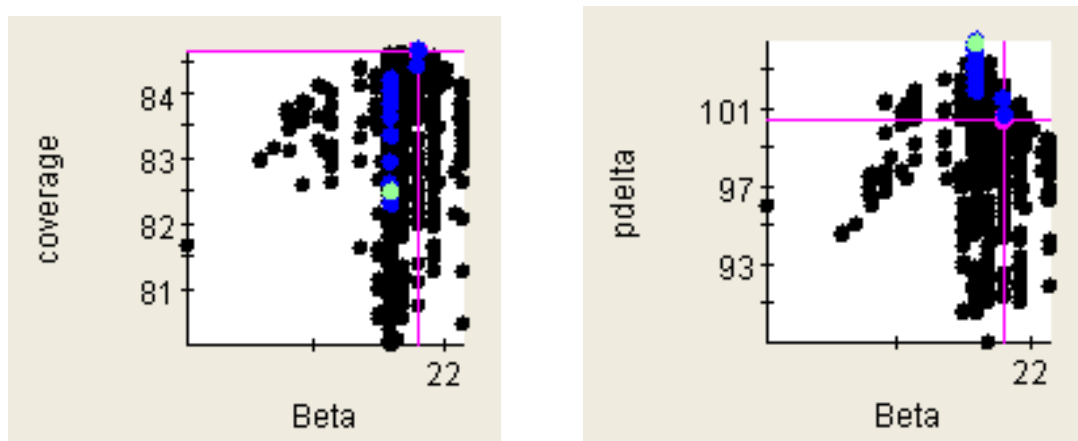


Figure 11(a)

Figure 11(a) suggests that β impacts both E and ΔP , and that the best designs from the perspective of both objectives are scattered around the $\beta = 20\%$ region.

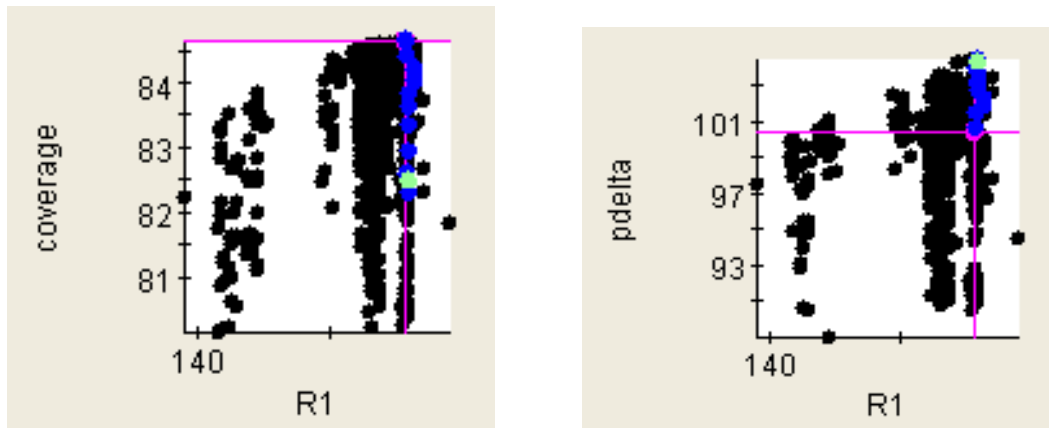


Figure 11(b)

Figure 11(b) suggests that large values of R_1 positively influence both E and ΔP , and that the best designs from the perspective of both objectives lie between 190 and 215.

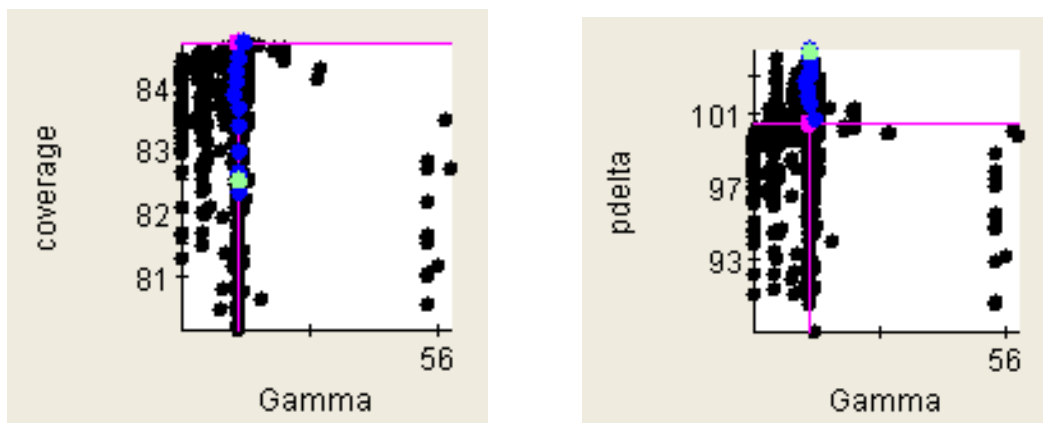


Figure 11(c)

Figure 11(c) shows that smaller values of γ are beneficial for both E and ΔP , and that the best designs result from values of γ between 40 and 48. There are also a few good solutions with values of γ that are around 56.

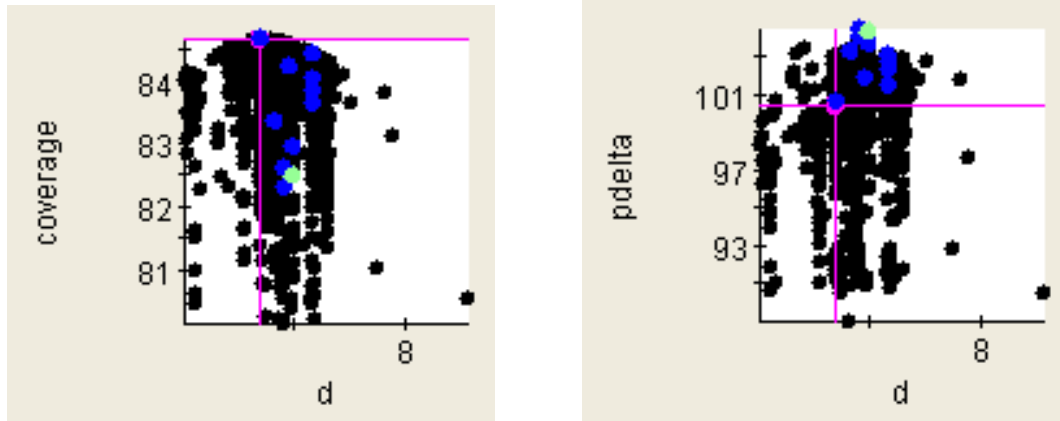


Figure 11(d)

Figure 11(d) suggests that intermediate values of d are desirable, and that the best designs from the perspective of both objectives lie between 3 and 6.

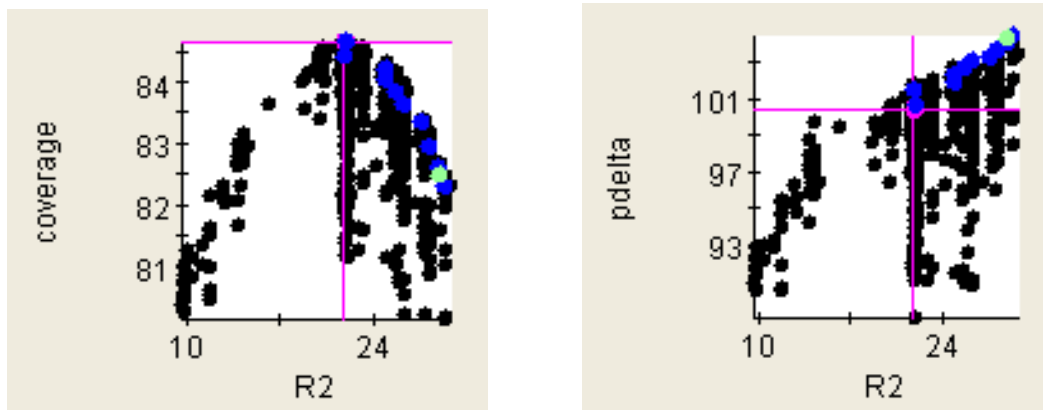


Figure 11(e)

Figure 11(e) illustrates that the Pressure Recovery goes up as R_2 increases, but the Evaporator Coverage peaks out at $R_2 = 20$. The choice of the value of R_2 then becomes a trade-off between the two objectives.

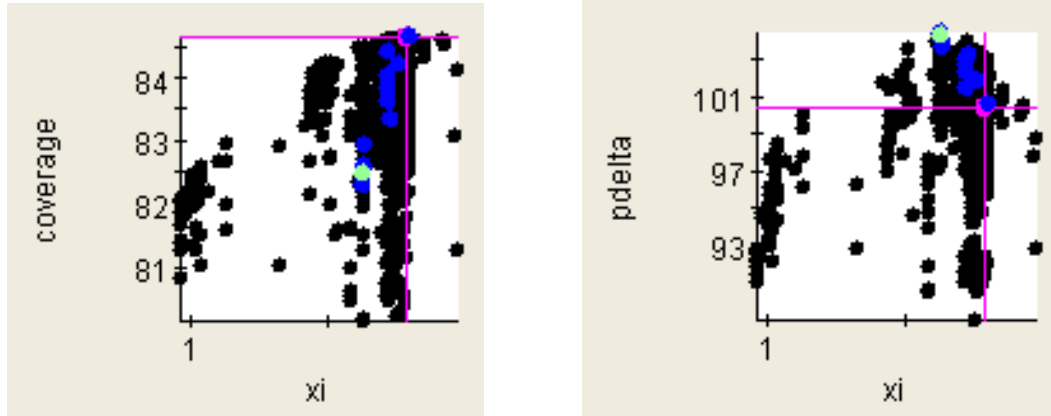


Figure 11(f)

Figure 11(f) indicates that the most favorable solutions from the perspective of both objectives have x_i values that lie between 10 and 17.

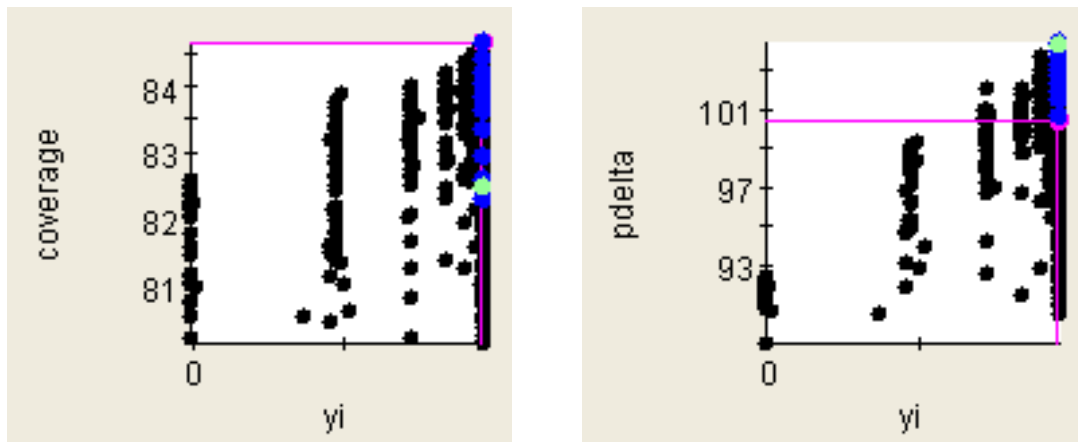


Figure 11(g)

Figure 11: Sensitivity Studies

Figure 11(g) indicates that the most favorable solutions from the perspective of both objectives have large values of y_i . The best designs all have values near the maximum of the range (17.3).

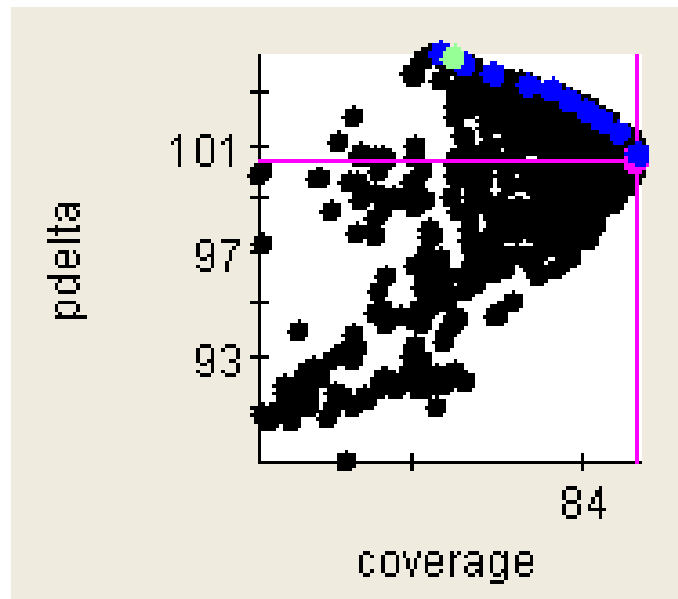


Figure 12: 2D Scatter Plot Showing the Pareto Front

The selection of the "optimal" solution involves examination of designs on the Pareto front (blue markers). Designs could be compared by weighting each objective suitably. However, in this study we select a design with the highest Evaporator Coverage since it also happens to have a favorable, although not a maximum, Pressure Recovery. The Pareto Front is shown in Figure 12, and the selected solution is reported in Table 3.

Since the optimization is based on interpolated Response Surface Models, we expect some error in any given function evaluation. Hence, it is advisable to recheck the optimal solution obtained by executing a CFD run. In doing this, we obtain $E = 82.4\%$ and $\Delta P = 107.9$ Pa.

OPTIMAL SOLUTION*	
Parameter	Min Value
β (deg)	20.63
γ (deg)	43.93
d	4.13
R_1	202.88
R_2	21.90
x_i	8.95
y_i	17.30
OBJECTIVES	
E(%)	84.66
ΔP (Pa)	100.70
CONSTRAINTS*	
x_E	36.78
y_E	102.62

* All length units in mm

Table 3: Optimal Solution

5. CONCLUSIONS

In this paper, we have presented a means to optimally design and locate vanes in the diffuser section of an automotive HVAC to achieve objectives relating to flow uniformity and energy efficiency (pressure recovery). CFD was used to quantify the impact of design changes on performance objectives. To accomplish the aforementioned task, we described a stepwise procedure which includes parameterization, morphing, meshing, CFD solution, and a number optimization related steps. We posed the formal optimization problem, specified the objective functions and constraints, and explored the design space for feasible optimum solutions with respect to the objectives. We found a family of solutions that were superior to the baseline design (one with no vane) in critical ways. As in a practical engineering design situation, a suitable configuration from this family of solutions was selected and discussed.

Nomenclature

β	Angle subtended by Arc 1 at Center 1
γ	Angle subtended by Arc 2 at Center 2
ΔP	Pressure recovery
ΔR	Difference in radii defined by equation (12)
θ	Angle defined by equation (12)
d	Trailing linear segment
E	Evaporator coverage
R_1	Radius of Arc 1
R_2	Radius of Arc 2
V_{avg}	Average velocity
x_A	x-coordinate of point A in Figure 4
x_B	x-coordinate of point B in Figure 4
x_C	x-coordinate of point C in Figure 4
x_D	x-coordinate of point D in Figure 4
x_E	Global x-coordinate of point D in Figure 4
x_i	x-coordinate of inlet
x_{o1}	x-coordinate of Center 1
x_{o2}	x-coordinate of Center 2
y_A	y-coordinate of point A in Figure 4
y_B	y-coordinate of point B in Figure 4
y_C	y-coordinate of point C in Figure 4
y_D	y-coordinate of point D in Figure 4
y_E	Global y-coordinate of point D in Figure 4
y_i	y-coordinate of inlet

y_{01} y-coordinate of Center 1

y_{02} y-coordinate of Center 2

REFERENCES

1. Jairazbhoy, V.A., Shahabi, M., and Barnhart, T., "Air Diffuser For A HVAC System", U.S. Patent Pending (2009)
2. Singh, R., "Automated Aerodynamic Design Optimization Process for Automotive Vehicle", 2003-01-0993, SAE World Congress & Exhibition, Detroit, MI (2003)
3. Wang., Huang, M., Lewitzke, C., Zhang, Q., and Yuan, C., "Multi Objective Robust Optimization for Idle Performance ", 2006-01-0757, SAE World Congress & Exhibition, Detroit, MI (2006)
4. ANSA version 12.1.5 User's Guide, BETA CAE Systems S.A., July 2008